Gamma-Rays Spectroscopy by Using a Thallium Activated Sodium Iodide NaI(Ti)

Ari M. Hamad[1] & Hiwa M. Qadr[2]

[1]Department of Physics, Faculty of Science and Health, Koya University, Erbil, Iraq
[2]Department of Physics, College of Science, University of Raparin, Sulaimanyah, Iraq
Correspondence: Ari M. Hamad, Koya University, Erbil, Iraq.
Email: ari.hamad@koyauniversity.org

Received: June 28, 2018 Accepted: August 26, 2018 Online Published: September 1, 2018

doi: 10.23918/eajse.v4i1sip99

Abstract: This paper focuses on two main parts. Firstly, some of the general properties of gamma radiations were studied, along with the performance characteristic of a sodium iodide NaI(Ti) scintillation detection system. Gamma ray spectra were generated for Cesium-137 and Cobalt-60 sources, illustrating the interaction mechanisms which result in partial or complete deposition of incident gamma radiation energy in the NaI(Ti) detector. The energy response of the system indicated to be linear function of deposition energy and the resolution ranged between 8.12% - 6.29% for voltages 500 – 750 volts. The values of intrinsic total, intrinsic peak and absolute efficiency were calculated and indicated to fall as a function of gamma-ray energy. The intrinsic efficiency values ranged between $11.1 \pm 0.004 - 4.2 \pm 0.006\%$ for energies of 511 - 1330 keV.

Secondly, the attenuation of gamma radiations was investigated, two materials such as zirconium and tungsten were tested and their attenuation coefficient was calculated to find that which of them has higher attenuation coefficient. The zirconium attenuation coefficient is $0.42 \pm 0.013\ cm^{-1}$, whereas the tungsten attenuation coefficient is $1.6 \pm 0.06\ cm^{-1}$. These results of this experiment suggest that tungsten is better shielding material than zirconium. This is expected because of the greater density and higher atomic number of tungsten, therefore, tungsten can attenuate gamma-ray more than zirconium.

Keywords: General Properties of Gamma Radiation, The Attenuation 0of Gamma Radiation, Sodium Iodide Nal (Ti), Linear Attenuation Coefficient

1. Introduction

High energy photons are one of the three main types of ionizing radiation resulting from natural radioactivity. They are an energetic form of electromagnetic radiation and occur in the form of gamma or X-rays. The distinction between them is based on their origin, where a gamma-ray is emitted from an excited nucleus and X-ray is emitted during atomic processes involving energetic electrons (Krane & Halliday, 1988). Since both are processes widely used in industry and medicine, it is important to be able to identify the major characteristics of various radioactive sources. This can be achieved by spectroscopy. A spectrometer is a tool to provide information about the energy and intensity of the radiation emitted from a source. In the case of gamma-ray detection, all or part of the original photon energy is transferred to an electron in the detector material producing a spectrum helping to understand the basic of photon interaction mechanisms as well as the characteristics of the detector material (Knoll, 2010).

How gamma radiations interact with shielding material as the progress through it, is also investigated

in this experiment. This is expected that results of relationship between gamma attenuation coefficient and material thickness will be exponential, because when the thickness of shielding material is increased, a number of gamma rays can pass through it will be decrease. Materials which have a high atomic number are more useful because the high density of materials increase the probability gamma radiation interaction with matter. As a result, the gamma radiation will lose all, or at least some of their energy, so only amount negligible of gamma radiations are getting through this materials (Krane & Halliday, 1988).

In the first part, this paper uses a thallium activated sodium iodide scintillator NaI(Ti) detector, a series of gamma ray sources and a multi–channel analyser (MCA) which is used to identify the major characteristics of some typical gamma-rays spectra and calculated some of the main features that characterize the performance of a spectroscopy system. And also in the second part, some lead blocks are used to avoid effective other radiation in the laboratory on our result. Furthermore, zirconium and tungsten plates are used and the attenuation coefficient for them has shielded (Hall, 2013).

2. Theory

For gamma-rays interactions with matters, there are primarily three process would happen depending on the energy of these photons (Knoll, 2010, Krane & Halliday, 1988). First of them is called photoelectrical absorption, which happens when an incident photon (has a low energy $\leq$ 200 keV experimentally) is absorbed by material then one of the electrons would be free after getting sufficient energy to release from the atom. Photoelectron process leads to the ionization in this atom (all the energy of the incident photon is deposited in the detector in this case).

The second one, when the incident photon faces an outer shell electron in an atom, this is a high probability for Compton scattering to occur, at minimum energy about 0.25 MeV. In this case, the energy after this interaction is shared between the recoil electron and the scattered photon. Also this energy depends on the angle of incidence according to the conversion laws and Compton derivation in 1923 (there is a partial deposition of the initial energy in the detector) (Knoll, 2010; Krane & Halliday, 1988).

The third type of these interactions which obviously occurs when the photon has a high energy (approximately 1.022 MeV and above) is known as a pair production (electron and positron) where the incident photon annihilates in the electric field around the nucleus and transforms to be pair product. The result of this interaction (electron and positron) is going to interact with matter by Coulomb interaction, but as the positron slows down it will annihilate with an electron to produce two back-to-back photons each with energy 0.511MeV (Knoll, 2010; Krane & Halliday, 1988). All these processes lead to the partial or complete transfer of the initial photon energy to electron energy within the detector material. This experiment were provided by a series of gamma-ray sources, a sodium iodide scintillator detector and a multi-channel analyzer (MCA) to identify the major characteristics of some typical gamma-ray spectra and calculates some of the main properties characterizing the performance of a spectroscopy system.

2.1 Sodium Iodide NaI(Ti)

The detector used in this experiment was thallium doped sodium iodide detector as shown in Figure (1). NaI(Ti) detector is the most widely detector use to detect gamma-rays. After sodium iodide

interacts with gamma rays at room temperature, a very little scintillation is generated. Whether pure sodium iodide is doped with an original amount (0.1 - 0.4%) of activator thulium, NaI(Ti) becomes more enough in generating light photons after gamma-rays interact with it. This interaction cause to ionize or excite NaI(Ti) molecules, by emitting light photons the high energy state go down to ground state again, and for 1kev energy about 20 - 30 light photons are generated.

The high atomic number of iodine (Z = 53) and high density of detector (3.67 g/cm^3) are two good reasons to choice NaI(Ti) detector to detect gamma-rays. However, the sodium iodide detector must be treating very carefully because its crystals are easy to break and hygroscopic. If the room temperature is changed suddenly, it would cause crack crystal, therefore it must be not changed quickly, and also some of lead blocks were used to form an enclosure to the detector and source radiations (Hubler, 1989).

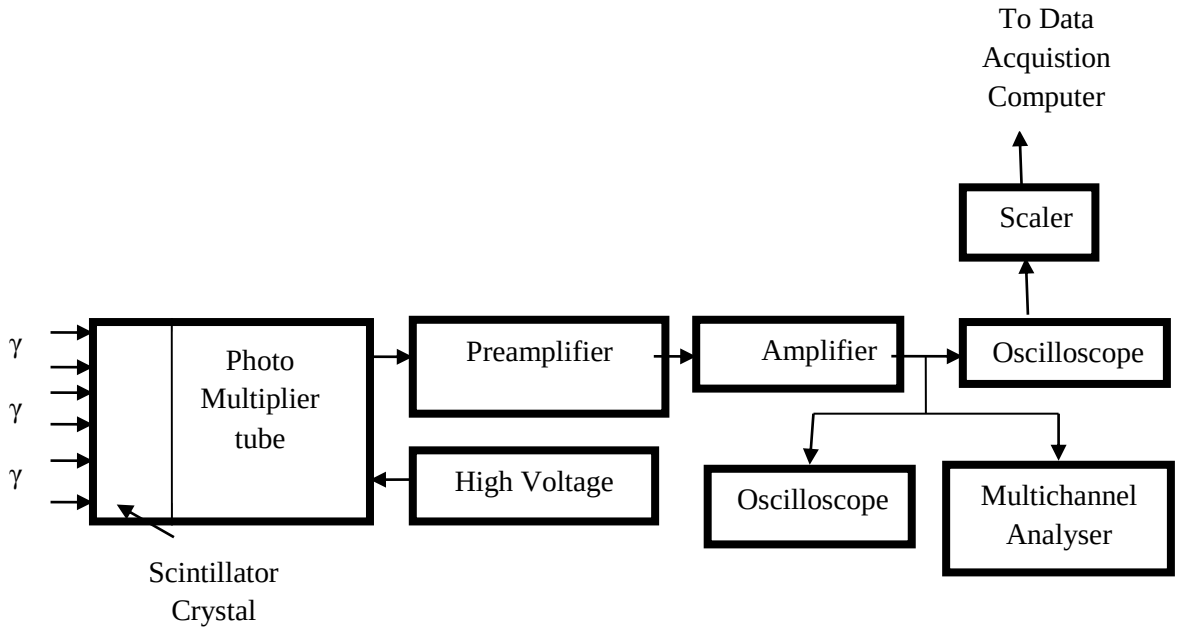

Figure 1: Schematic of NaI(Ti) Detector

2.2 The Energy Resolution

The relevant detector type must be used for spectroscopy and there are several of these must be evaluated the specific characteristics of each detector so as to use the correct one. One feature which is important in every spectroscopy system is the exponential or linear relationship between the magnitude of the output pulse and the photon energy deposited in the detector which is shown by plotting the number of known sources incident photon energies against the channel number of the peak centroid in each spectrum. Equation (1) shows the energy resolution (R) which is defined as the detector's ability to resolve little alterations in the energy of incident photons. ($FWHM$) is the full width at half maximum and it is known as the width of the distribution at half of the level of the peak and where H_0 represents the peak centroid channel number.

$$R = \frac{FWHM}{H_0} \times 100\% \quad (1)$$

If the resolution value is small this means that a pair of energy peaks closes in proximity can be more easily identified by the detector. However, if the detector has a large value for resolution it will create one peak for both energies. Energy peak for any given detector is estimated as a Gaussian Curve. The primary contributor to peak broadening is statistical variability in the number of charge carriers generated in the detector for a given deposition energy. They could be defined by Poisson Statistics, the resolution (R) is related to the peak gamma-ray energy (E_γ) as follows (Knoll, 2010):

$$R \propto {E_\gamma}^{-1/2} \tag{2}$$

2.3 The Efficiency

The efficiency of photons being detected is also an important factor to consider. It may be defined in several ways, either absolute efficiency values or intrinsic efficiency values. The values of total efficiency (ε_t) produced depend on the properties of the detector. They will also vary as a function of the counting geometry for example: the distance from the source to the detector. In equation (3) it is defined as the total number of counts per unit time (C_t) over the entire recorded spectrum, apart from the background rate. The number of gamma–rays emitted by the source per unit time is expressed as N:

$$\varepsilon_{abs} = \frac{\text{no. of recoreded pulses}(C_t)}{\text{no. of emitted photons by a sources}(N)} \tag{3}$$

Where N is the current activity of the source, D_s and the fractional number of gamma-rays emitted per disintegration, I_γ (E_γ):

$$N = D_S\, I_\gamma\, (E_\gamma) \tag{4}$$

ε_i Is the intrinsic total efficiency, does not include the counting geometry as an inherent factor. This is because the solid angle subtended by the detector (Ω) is taken into consideration in its definition. Therefore, it is simply a function of the detector material.

$$\varepsilon_i = \frac{no.of\ recoreded\ pulses}{no.of\ incident\ p\square otons\ on\ a\ detector(N_\gamma)} \tag{5}$$

N_γ is defined as:

$$N_\gamma = \frac{\Omega}{4\pi} N \tag{6}$$

ε_p is the intrinsic photo peak efficiency, only considers the full energy peak region concerned in the calculation which is useful as it does not take into consideration any regions where there may be scatterings from other objects nearby or electrical noise. In equation (7), C_p is the number of counts in the photo peak corresponding to energy ε_γ per unit time (Knoll, 2010).

$$\varepsilon_p = \frac{c_p}{N_\gamma} \tag{7}$$

2.4 Attenuation Coefficient

Attenuation is the removal of photons form a beam of gamma rays as it passes through matter. Attenuation is caused by absorption, scattering and pair production of the primary photons. At low energies (< 26 keV) the photoelectric effect dominates the attenuation processes. However, when higher energy photons interact with low Z materials, Compton scattering dominate of attenuation. Also at very high photon energies (> 1.02 MeV), Pair production contributes of attenuation. There are two types of attenuation coefficient.

First, the fraction of beam of gamma rays which is absorbed per unit thickness of material is called linear attenuation coefficient (μ). Typically expressing in unit of inverse centimeter, the number of photons removed from the beam traversing a very small thickness (Δx) can be expressed as:

$$n = \mu\, N\, \Delta x \tag{8}$$

Where *n* is then number of photons absorbed from the beam, and *N* is the number of photons incident on the materials.

For a mono-energetic beam of photons incident upon either thick or thin a slabs of material, an exponential relationship exists between the number of incident photon (N_0) and those are transmitted (*N*) through a thickness (*x*) without interaction;

$$N = N_0\, e^{-\mu x} \tag{9}$$

The linear attenuation coefficient is the sum of the individual linear attenuation coefficient for each type of interaction:

$$\mu = \mu_{p\square oto\ electic\ effect} + \mu_{compton\ scatter} + \mu_{pair\ production} \tag{10}$$

For a given thickness of material, the probability of interaction depends on the number of atoms the gamma rays encounter per unit distance. The density (ρ in g/m^3) of materials effects this number, also the linear attenuation coefficient is proportional to the density of material (Bushberg & Boone, 2011).

Second, mass attenuation coefficient is the normalizing linear attenuation coefficient to unit density. For a given thickness, the probability of interaction is dependent on the number of atom per unit volume. This dependency can be overcome by normalizing the linear attenuation coefficient for the density of the material.

$$\left(\frac{\mu}{\rho}\right) = \frac{\text{linear attenuation coefficient } (\mu)(\text{m}^{-1})}{\text{density of material}(\rho)(\frac{\text{kg}}{\text{m}^3})} \tag{11}$$

The units of mass attenuation coefficient are (m^2/kg) (Bushberg & Boone, 2011).

3. Experimental Procedure

Figure (2) shows the basic setup of the apparatus for this experiment. In this experiment a Cs-137 sources was chosen to find energy resolution of the NaI(Ti) detector. The source was placed a distance (9 cm) from the face of the detector. An ionization chamber was used to record the radiations from this source. This ionization chamber is very advanced device which contains two electrodes and a gas. They create an electric field when the radiation from source incident detector causes ionization within gas. An ion and electrons produce as a result of this reaction. These ions are attracted to the anode and electrons to the cathode. Furthermore, there is a current because of the flow of charge that can be measured. This kind of detector does not contain an amplifying component so count rate is not defined.

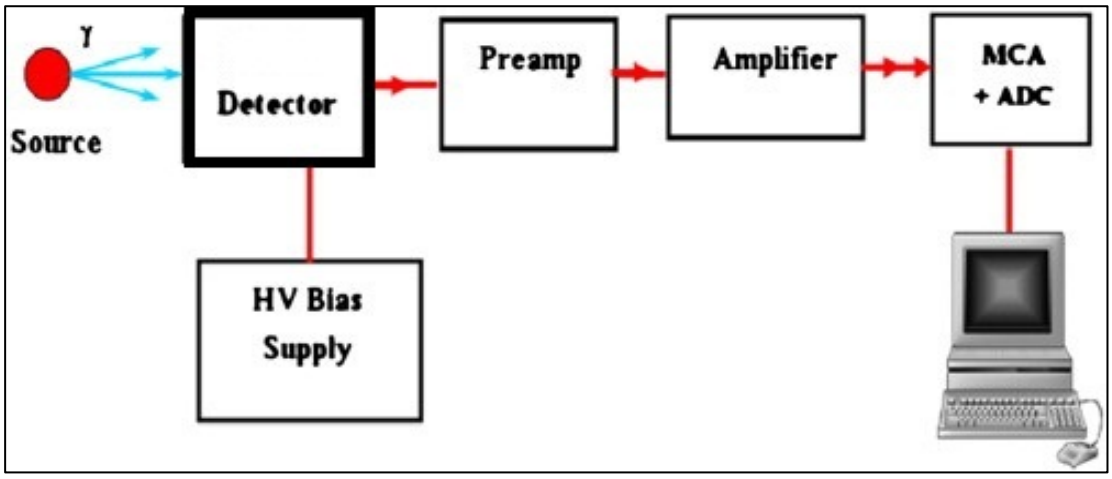

Figure 2: Experimental setup

The NaI(Ti) detector was put in place. At the binging an initial measurement with no shielding in place was taken. The electronics converted the reading from the detector to an electrical pulse. This electrical pulse is then changed to a digital pulse and recorded by the computer. The maestro program analyses the spectrum. And then spread the energy spectrum over a range a two thousands of channels which are proportional with energy. They let us read the width and position of the peak (Cs-137 has only one peak). The software lets for an area of interest to be chosen and the peak information order displays the specific of peak. There is two or one region of interest in this experiment (because in this experiment Cs-137, Na-22 were used which have one peak, and Co-60 was used which has two peaks) such as the Compton continuum and the photopeaks which are the characteristic energy for the radioactive source. In the case of Cs-137 one peak was expected to be found at the point in the spectrum that corresponds to energy of 661 keV, and for the Co-60 tow photopeaks were expected to be found in the spectrum which related to energies of 1170 KeV and 1330 keV. The gamma ray is emitted from the Co-60 source and beta decay is then Co-60 to Ni-60.

For the energy resolution, the measurements were taken with various volts (500, 550, 600, 625…. 750 volt) at constant distance and time (300 seconds). After obtained measurements, the energy resolution of the NaI(Ti) detector was studied by recording centroid energy *FWHM* and centroid channel number, for the peak collected from the Cs-137 source . H_0 & *FWHM* were found by using peak fir program and calculated energy resolution by using equation (1).

Another part of this experiment is energy calibration which is important to check the detector

measurement and to be accurate (to select the energy that close to standard and to decrease the rate error in the measurement) because of the convert in the feature of the equipment's and their different parts (Knoll, 2010; Krane & Halliday, 1988).

To find the calibration in this experiment some steps were performed. Firstly, a number of gamma radioactive sources were chosen such as (Cs-137, Co-60, Eu-152) in order to make out the linearity of the energy response for the NaI(Ti) detector, then they were replaced (9 cm) from the face of the detector and the power supply was set at (700 volt) for (500 seconds). After that the peak channel was calculated by eye and using the peak report function on the MCA.

The difference types of detector efficiency were determined by using a Cs-137 radioactive source to collect a spectrum. The source was placed (5 cm) from the detector for (300 seconds), and then the interesting area of the whole spectrum was measured. Moreover, the net count rate over the collection time was obtained after selecting the full energy photo peak. This measurement along with the activity of the source, which was calculated by using equation (4) this procedure, was repeated for Na-22 and Co-60.

For attenuation coefficient some different type of materials were used and also a strong Cs-137 radioactive source was used. A lead plate was placed in front of the Co-60 source. A Vernier Cappiler was used to measure the thickness of the plates. As the calipers were subject of the error of parallax and the plates were not of uniform thickness. Three individual reading were taken for each thickness and averaged. This was done for five lead plates. When a new plate was inserted, a new spectrum was taken, and the count rate of interest area included in the peak was measured at each thickness. The natural logarithm (ln) was taken for photopeaks area at each thickness. The number of cunts are proportional these natural logarithm values and as a result of intensity. The graph of the plate thickness against natural logarithm of count rate was plotted, and linear attenuation coefficient was given by the slope of this graph for zirconium or tungsten. The same method and steps was repeated for a series of zirconium and tungsten plates.

4. Results

4.1 Gamma Radiation Spectra

Figures (3 & 4) provide the gamma-ray spectra collected for the Cs-137 and Co-60 radioactive sources. The characteristic properties for each source are labelled and will be discussed in conclusion.

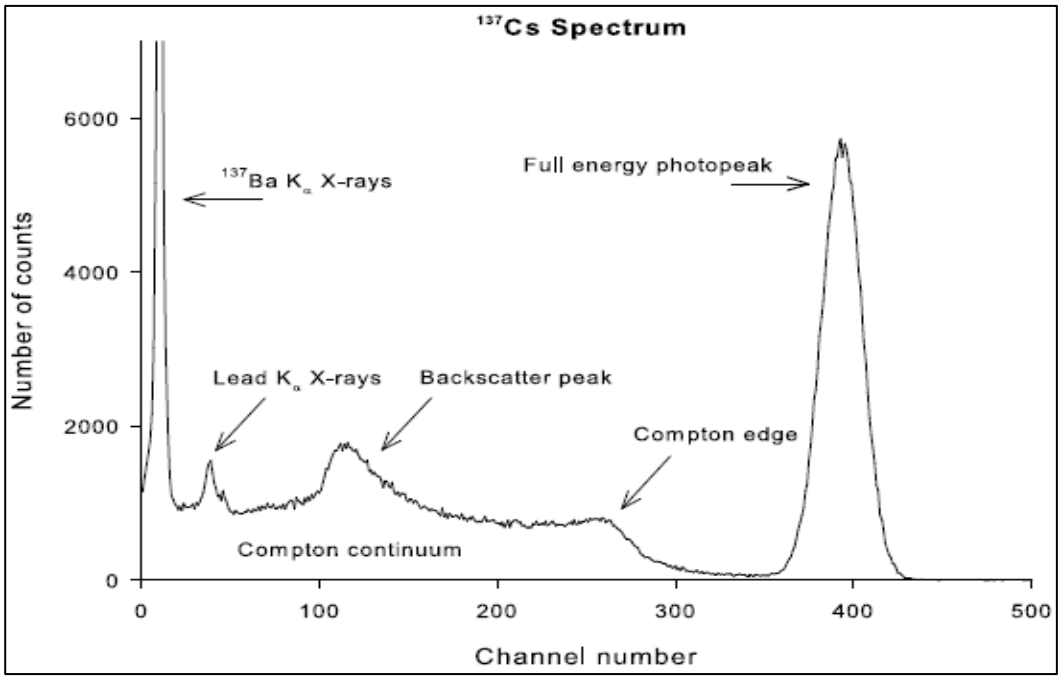

Figure 3: Characteristic features of a Cs-137 gamma emitter

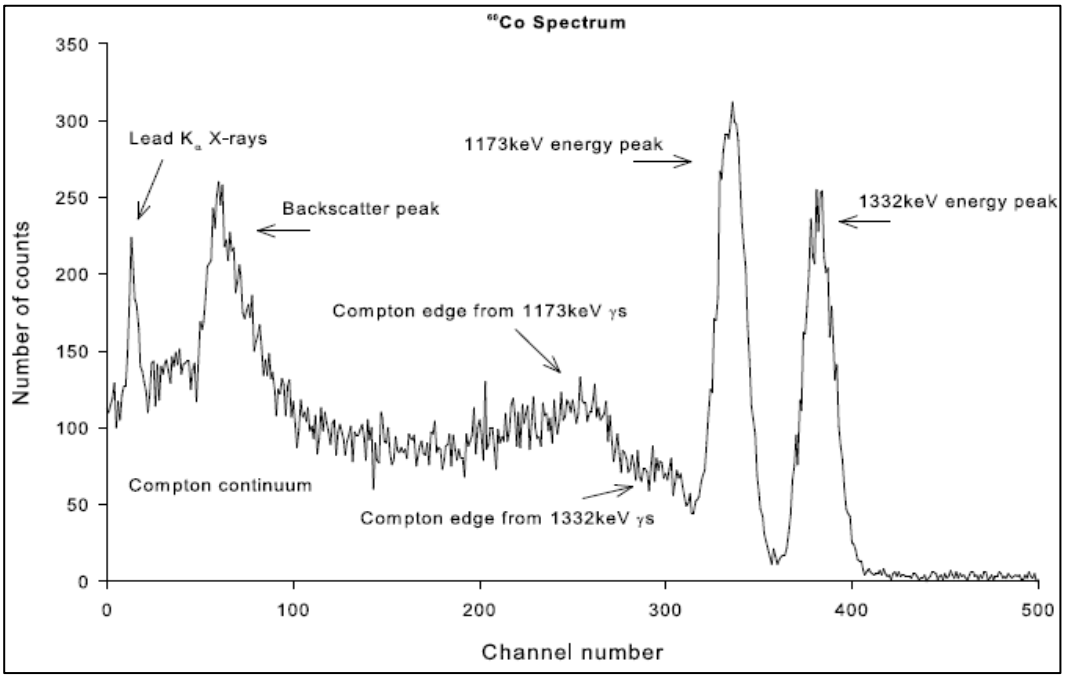

Figure 4: Characteristic features of Co-60 gamma emitter

4.2 The Characterization of NaI(Ti) Detector

Figure (5) shows the gamma energy sources against the peak channel number for (Cs-137, Co-60 and Eu-152) sources, the equation (7) was used to find the error in the peak centriod channels (±4

channels). A linear relation is generated for the gamma energy with a gradient of 0.7168 ± 0.003 channels/keV, also for the Y-intercept was calculated to be 47.7 ± 0.4 channels.

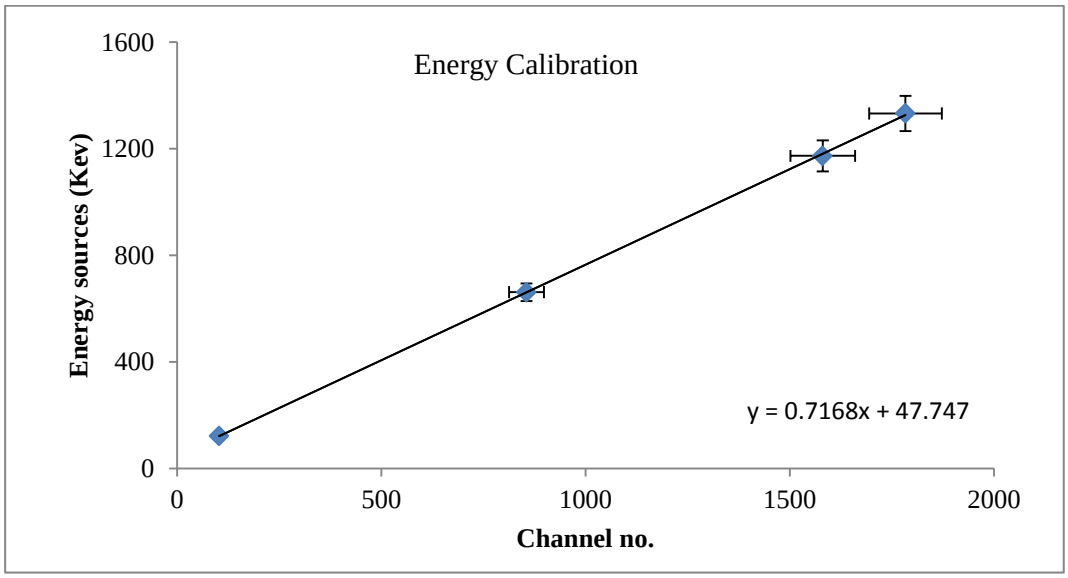

Figure 5: Linear energy response of the NaI(Ti) detector

Figure (6) shows the energy resolution plotted against voltages. The energy resolution of the detector ranged between 8.12% - 6.29% for voltages 500 – 750 volts. The voltage of the detector was found to be 700 voltage because the energy resolution of the NaI(Ti) detector was at low point when the detector voltage was at 700 voltage.

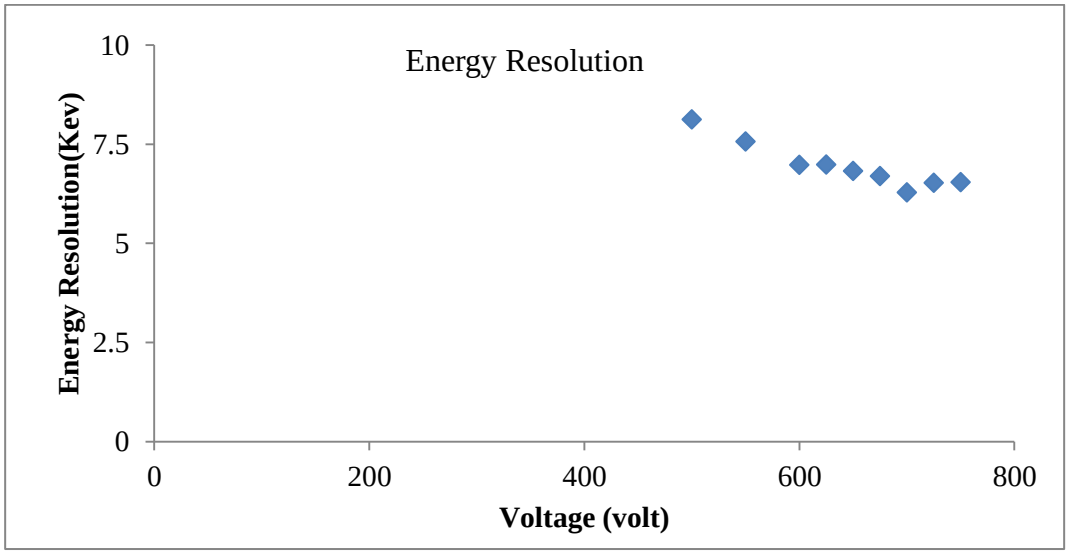

Figure 6: Energy Resolution of NaI(Ti) detector

From the Table (1), the equation (3-7) were used, count rate in the photo peak and the net count rate over the full energy spectrum were measured to calculate the absolute, intrinsic and photo peak intrinsic efficiency for the NaI(Ti) detector at various gamma ray energies such as (Cs-137, Co-60, Na-22) sources, and also the current activity of sources was calculated by using equation (4). Figure (7) shows the gamma-ray energy plotted against the intrinsic phototpeak efficiency.

Table 1: Efficiency as a function of gamma-ray energy

Sources	Eγ (keV)	N (Bq)	net area(count rate)	Absolute eff.	Solid angle	intrinsic efficiency	ε_i (%)
Cs-137	661	155763.8	825846	0.0075	0.85	0.11	11.1 ± 0.004
Na-22	511	3109.9	32364	0.031	0.85	0.46	46.3 ± 0.001
	1275	3109.9	5082	0.0027	0.85	0.04	4.1 ± 0.002
Co-60	1170	1479.8	3421	0.0039	0.85	0.057	5.7 ± 0.004
	1330	1479.8	2540	0.0029	0.85	0.042	4.2 ± 0.006

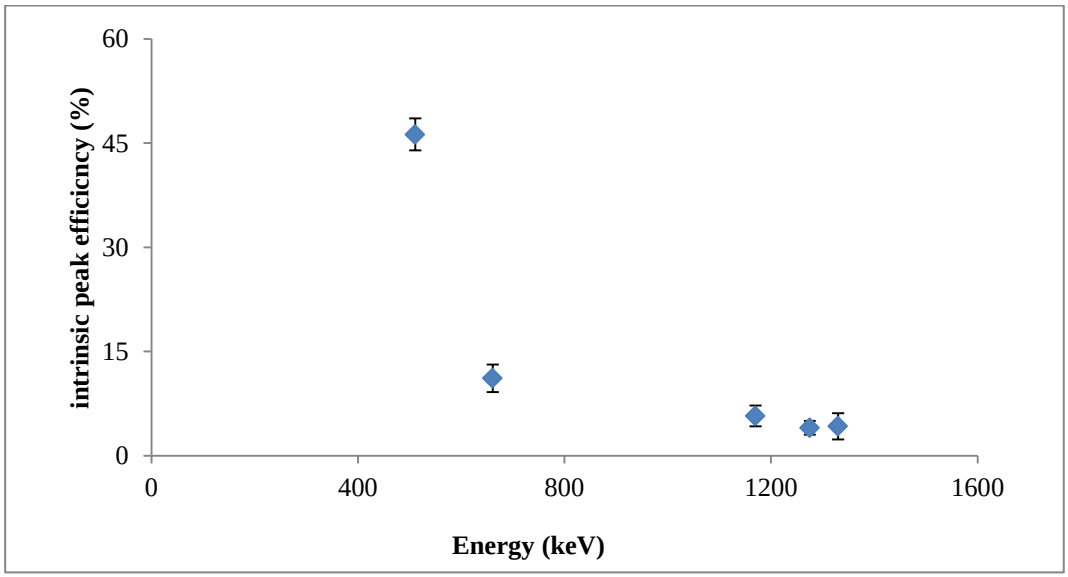

Figure 7: Intrinsic peak efficiency for the NaI(Ti) detector

4.3 Gamma Attenuation Coefficient

The radiations that form the Cs-137 were measured by the ionization chamber. At the binging, Gross count rates were 1144575 without out shielding, but then count rate decreased with increase thickness of shielding such as (zirconium, tungsten), it will be discussed in conclusion.

$$N = N_{0\,e^{-\mu x}} \tag{12}$$

$$\ln(N) = \mu x + \ln(N_0) \tag{13}$$

Equation 12 was used to rearrange equation (13), also it lets for fitting the data linearly. Thus, the

slope of this figure gives us the linear attenuation coefficient for zirconium (μ_{zr} = $0.42 \pm 0.0013\ cm^{-1}$). Figure (8) provides the thickness of the zirconium plates against the natural logarithm of Gross area counts for full energy peak.

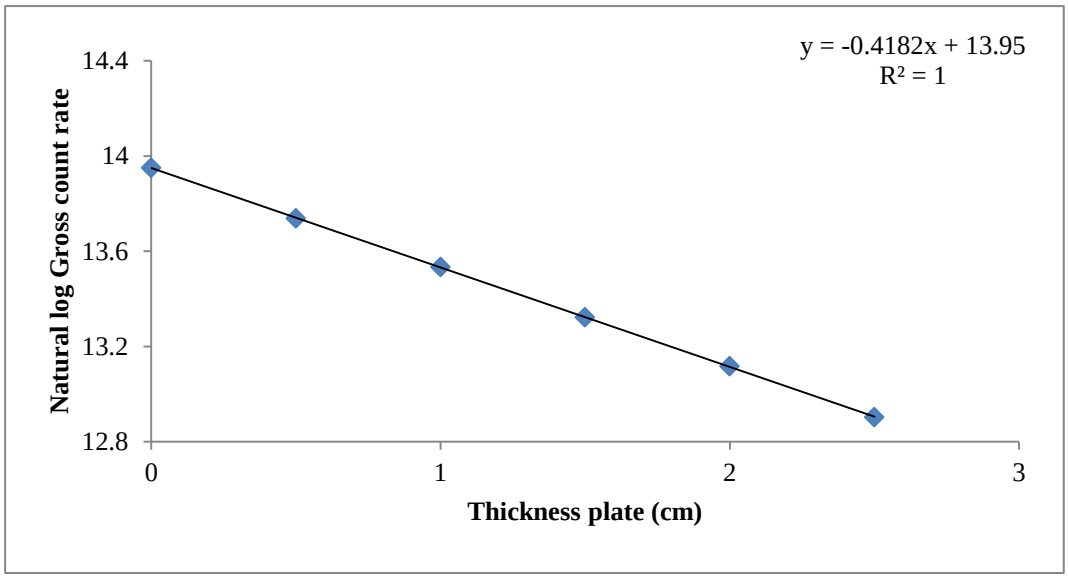

Figure 8: Zirconium plate thicknesses against natural log of count rate

Figure (9) shows the thickness of the tungsten (wolfram) plates against the number of counts for full energy peak. This figure was fitted by using equation (12), and lets for fitting the data exponentially. Thus, the slope of this figure provides the linear attenuation coefficient for tungsten ($\mu_w = 1.6 \pm 0.006\ \text{cm}^{-1}$).

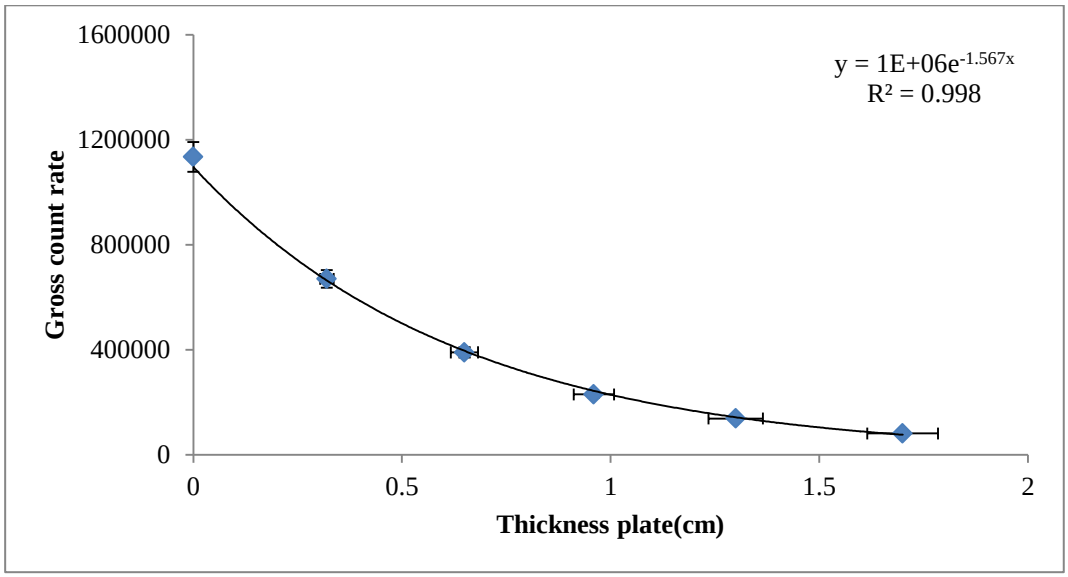

Figure 9: Tungsten plate thicknesses against Gross count rate

5. Discussion and Conclusion

A number of the performance characteristic of sodium iodide detector NaI(Ti) and the general properties of the gamma ray spectra have been illustrated in this experiment. Firstly, Figures (3) and

(4) provide the gamma spectra got from Cs-137 and Co-60 radioactive sources and all of the main properties discussed in theory are labelled. A lead plate was used with NaI(Ti) detector, so the characteristic of X-ray signals appeared at 74.2 keV for both spectra in Figures (3 & 4). The Figure (3) labels an extra feature from Ba-137 K_α X-rays; we can understand this peak from the decay scheme of cesium-137. Although Cs-137 β-decays to an excited state of Ba-137 93.5% of the time, the associated 662 keV gamma-rays is observed in only 85% of disintegration. This is because of a competing mechanism as known an internal conversion, which happens when the energy transition between two different energy levels are transferred immediately to one of the orbital electrons, as a result the electron will be ejected from the atom. Therefore, an X-ray characteristic of the element is generated. Figure (4) provides a similar spectrum, although full energy peaks and two Compton edges exist. This is because of the fact that cobalt-60 generates two gamma-rays with 100% intensity at energy 1173 keV and 1332 keV. Another peak would also be expected to be present, which is sum peak, at energy 2505 keV. It is as a result of two gamma-rays full of energy reaching the NaI(Ti) detector simultaneously. But the single was used as a minimal in this detector, so it is not present in the figure.

Figure (5) provides information about energy calibration and also shows a linear relation between incident gamma energy and the peak channel number, during this experiment there were few differences between the reading taken by eye and those generated by (MCA) peak report, with errors of the order 1 - 2% in each case. Ideally in a semiconductor detector a smaller difference would be desirable. Although the general trend provide that the output pulse is proportional to the amount of energy deposit in the NaI(Ti) detector by incident photon radiations. The range of radioactive sources were used in this experiment shows a constant relationship over a wide range of energies.

Figure (6) shows the energy resolution of the NaI(Ti) detector as a function of gamma energy. Energy resolution values ranged between 8.1% at 500 volt to 6.53% at 750 volt. A small value of energy resolution means that the detector is better able to identify two energy peaks which close to each other, whereas the NaI(Ti) detector with a large resolution value produces on peak for two energies. Because of this reason, in this experiment a small value of energy resolution was chosen which is 6.3% at 700 volt, therefore the voltage of NaI(Ti) detector was 700 voltage for all section in this experiment. The results from this experiment indicate that the NaI(Ti) detector has a very bad energy resolution compared with semiconductor detector namely HPGe, typically, which has a value range between 0.02 - 2.5% (Molnar, 2004).

In the Table (1), the intrinsic peak, intrinsic total, absolute total efficiencies were calculated for the Na-22, Co-60 and Cs-137 radioactive sources to show how these efficiency values are different as a function of incident gamma radiation energy. The current activity for each source was calculated by using equation (4) and also the net count rate was measured in each peak as well as over the whole spectra. The all value of efficiencies fell as a function of rising gamma radiation energy with the intrinsic total efficiency range between $11.1 \pm 0.06 - 4 \pm 0.04\%$ and the absolute total efficiency values were between $0.75 \pm 0.04 - 0.27 \pm 0.02\%$ for energies of 511 – 1275 keV as shown in Table (1). These result shows that at high gamma ray energy rang all of the efficiency values were low, whereas when the gamma ray energy is low, the value of these efficiencies was high. This is expected at lower energies when the photons spend more time in the vicinity of the NaI(Ti) detector material and as a result have a higher possibility of interaction, but at higher energies, it is opposite. The counting statistics in each spectra cause to main error contribution in each case. The Figure (10) shows the intrinsic efficiency against gamma energy. The function generated is not linear but future

experiments could focus more and use more radioactive sources over a wider range of energy values.

The linear attenuation coefficient for tungsten is higher than of zirconium, this is expected because of the greater density and higher atomic number of tungsten. The results of this experiment suggest that tungsten is better shielding material than zirconium because tungsten can attenuate gamma ray more than zirconium. The result of this experiment also shows that if the density of zirconium is taken to be 6570 kg.m^{-3} (Sheriff & Rook, 1990) then the mass attenuation coefficient of zirconium can be taken to be $6.4 \pm 0.004 * 10^{-5}$kg. m^{-2}. Whereas if the density of tungsten is 19600 kg. m^{-3} (Lindquist & Paddick, 2007) then the mass attenuation coefficient for tungsten obtained is $8.2 \pm 0.004 * 10^{-5}$ kg. m^{-2}. The evidence of this study indicates that the mass attenuation coefficient a material is inverse to density of the material, however the attenuation of gamma-rays is proportional and depends on density and atomic number of the material, as given in the result of this paper. The linear attenuation coefficient of tungsten is greater than zirconium, due to the atomic number (Z = 74) and density of tungsten is higher than zirconium (Z = 40) (Bushberg & Boone, 2011).

This paper will serve as a base for future studies. Firstly, future experiments could concentrate more and use more radioactive sources over wider range of energy values to find good efficiency of NaI(Ti). Furthermore they could focus more on how gamma radiation interacts with high atomic number and density and more dense materials. However, it may not be of more interest in areas where gamma rays are used directly. But this would be more applicable to shielding; it will encourage finding good shielding material to storage water material which nowadays is a big problem in the world. By increasing atomic number and density then gamma rays interact with more atom in a material, thus less gamma radiation can pass though material.

References

Bushberg, J. T., & Boone, J. M. (2011). T*he essential physics of medical imaging*. Lippincott Williams & Wilkins.

Hall, R. G. (2013). Nanoscintillators For Radiation Detection. https://rc.library.uta.edu/uta-ir/bitstream/handle/10106/11861/Hall_uta_2502M_12277.pdf?sequence=1&isAllowed=y

Hubler, G. (1989). Fundamentals of ion-beam-assisted deposition: technique and film properties. *Materials Science and Engineering: A*, 115, 181-192.

Knoll, G. F. (2010). *Radiation detection and measurement*. John Wiley & Sons.

Krane, K. S. & Halliday, D. (1988). *Introductory nuclear physics*. Wiley New York.

Lindquist, C. & Paddick, I. (2007). The Leksell Gamma Knife Perfexion and comparisons with its predecessors. *Operative Neurosurgery*, 61, ONS-130-ONS-141.

Molnar, G. (2004). *Handbook of prompt gamma activation analysis: With neutron beams*. Springer Science & Business Media.

Sheriff, D. & Rook, D. (1990). Wood density and above-ground growth in high and low wood density clones of Pinus radiata D. Don. *Functional Plant Biology*, 17, 615-628.